Chapter 8
A Novel Method to Attach Membranes Uniformly on MAV Wings

Yaakov J. Abudaram, Sean Rohde, James Paul Hubner, and Peter Ifju

Abstract Highly compliant wings have been used for MAV platforms, where the wing structure is determined by some combination of carbon fiber composites and a membrane skin, adhered in between the layers of composite material. The wing topology can be tailored to obtain the desired change in aerodynamic performance through passive shape adaptation. Pre-tension of the membrane plays a major role in the static and dynamic response of membrane wings and controls the overall deflections. In the past, the methods used to apply pretension when fabricating MAV wings were rudimentary. A new technique of attaching membranes firmly on wing structures is introduced, which involves the application of a technology known as corona treatment combined with another repeatable method of tensioning silicone membranes on any given frame geometry. Corona treatment provided a means of increasing adhesion of silicone on carbon fiber through the use of a high-frequency high-voltage air plasma discharge. The silicone membrane is co-cured with carbon fiber under vacuum pressure at an elevated temperature. After cool down, the membrane is tensioned.

8.1 Introduction

Micro air vehicles, or "MAVs", are defined as an aircraft with a maximum size of 15 cm and are capable operating at speeds of 25 mph or less [1]. Despite their size, MAVs are expected to be able to carry a payload of 20 g for 20–60 min [2]. The idea is a design of a small, reliable, and an inexpensive vehicle that can survey a remote area that is not easily accessible with ground transportation [3]. For example, a MAV may be placed under a missile and jettisoned right before the missile reaches the targeted area to send images of the damage to the base. A variety of wings may be envisioned for these vehicles, such as fixed, rotary, and flapping while this work is concerned with the fixed type [4].

The vehicle may greatly suffer in terms of controllability and range of operation when flying outdoors due to wind gusts [5]. Similarly, operation of MAVs can be highly challenging when flying indoors because of the air ducts and vents. Two types of mechanisms are introduced to overcome this issue: utilizing a passive mechanism or an active mechanism. Latter idea can be highly complex and expensive and in most cases a passive mechanism may be sufficient enough for a given mission. The wing design can be modified depending on the desired change in aerodynamic performance through passive shape adaptation [6].

A perimeter reinforced MAV wing fabricated at University of Florida is shown in Fig. 8.1a. Perimeter of the membrane skin is restricted by the thin strip of carbon fiber. This configuration allows the membrane to bulge out at increasing angles of attack and higher speeds. Result is an increase in lifting efficiency with high C_L and low $C_{M\alpha}$ [4]. Figure 8.1b shows a batten reinforced wing where the trailing edge of the membrane is not constrained while the membrane is supported by three

Y.J. Abudaram (✉) • S. Rohde • P. Ifju
University of Florida, Gainesville, FL 32607, USA
e-mail: abudaram@ufl.edu

J.P. Hubner
University of Alabama, Tuscaloosa, AL 35487, USA

Fig. 8.1 Two different types
of airplanes that are fabricated
in micro air vehicle laboratory
at the University of Florida
(**a**) Perimeter Reinforced
(**b**) Batten Reinforced
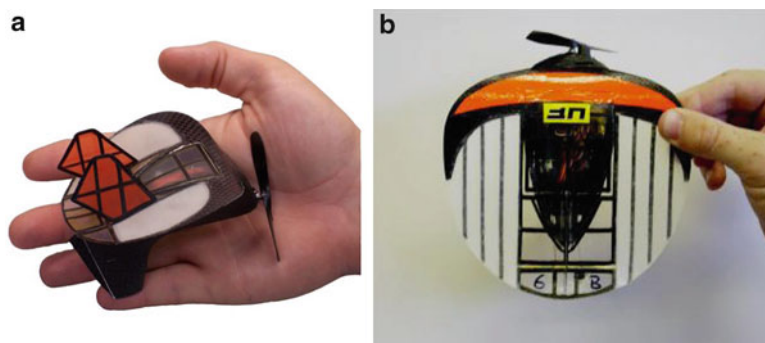
two-layer unidirectional carbon fiber battens on each side of the wing. In this case when the MAV flies into a head-on gust, the trailing edge flexes upwards resulting in adaptive washout. The effect is a near-constant lift history with exceptional smoothness even in gusty conditions [7].

Numerous materials have been found applicable to be used as membranes on the aforementioned wing geometries [3]. Most widely used material has been latex due to its benefits (elongation properties, ease of fabrication, and passive shape adaptation [8]). Nevertheless, latex material does not have appreciable shelf life and degrades at a rapid rate under hot and humid conditions. Further disadvantages include the degradation of the material when touched or contacted with various fluids, such as alcohol, oil, or water [9]. Rudimentary methods used to be applied when applying the latex membrane on wing skeleton: the latex rubber was stretched to be pinned on a particle board and adhered with glue on the carbon fiber wing; thereby, the pre-tensions achieved on various models were neither repeatable nor measurable.

Static and dynamic response of membrane wings are significantly affected by the pretension. Overall deflections (amount of camber on a perimeter reinforced wing, trailing edge vibration and reflex on a perimeter reinforced wing, etc.) are controlled by the tightness of the membrane [9].

The current work focuses on altering the material from latex to silicone to vastly improve durability. A method to quantify the pretension is discussed in detail by Abudaram et al. [9], in which this paper will use a similar technique to measure the strains developed on a silicone membrane that is co-cured with carbon fiber composite in an oven. One drawback is poor adhesion of most adhesives to silicone rubber. The solution to this manufacturing problem is corona treatment. The goal of surface treatment is to alter the mechanical properties at the surface of the silicone material to achieve a particular desired characteristic. In the cases to be considered, the primary characteristic of the materials is its surface energy. Surface energy affects the ability of a material to bond to an outer layer, which can be increased by roughening the surface area.

Despite being an integral part of the manufacture of polymers, corona treatment is rarely discussed. The name corona comes from the halo like appearance it gives off. Early tests confirmed its existence, but the potential for commercial application was not fully realized until the 1950s. Although this unique technique has been used for over 50 years, the principle behind how corona treatment improves adhesion is not entirely understood. Four generally accepted theories remain behind how the air plasma affects the surface of the substrate. The formation of electrets, the removal of weak boundary layers, an increase in roughness caused by small pits, and the deposition of chemically charged hydroxide ions on the surface are the most common explanations [10]. Electrets are non-conducting substances, like polymers, which become partially charged when placed under an electric field. The air plasma is generated by creating a steep electrical gradient. The surface to be treated is placed near the air plasma so the electrets hypothesis is a possible explanation. The weak boundary layer theory asserts that failures of adhesives are primarily the cause of weak boundary layers, which can be the result of air pockets between the surfaces or impurities in the adhesive [11]. The third explanation for the improved adhesion of surfaces treated with air plasma is attributed to an increase in roughness. Common practice is to sand a surface down before an adhesive is to be applied in order increase the strength of the bond. The theory behind this is that the surface energy increases as the surface area increases. A change from a flat surface to a rough one increases the surface area of the material on the microscopic level while on a macroscopic level the material appears as the same size. The increased surface energy means that a greater energy must be applied to the system to break the bonds and cause fracture. The fourth theory of how corona treatment improves adhesion to materials is that the air plasma results in a separation of molecules from their electrons, which creates an abundance of charged free radicals to be deposited on the nearest surface. In the case of these applications this surface is the substrate being altered. The deposited charged particles now exhibit a strong static attraction to foreign bodies. Since these theories are not mutually exclusive, the actual mechanism may in fact be a combination of all four of the aforementioned causes.

To analyze how effective the corona treatment is between silicone and prepreg carbon fiber layers a width tapered double cantilever beam test will be applied. Jyoti et al. [12] has pointed out the difficulty of measuring the crack length during dynamic fracture toughness testing on double cantilever (DCB) specimens. A practical solution was found by Daniel et al. [13] with the study of the quasi-static Mode I energy release rate of width tapered specimens, which allowed the energy release rate to be independent from the crack length. There also exists a similar technique of thickness tapered DCB; however, this type is cumbersome to manufacture.

8.2   Experimental Techniques

8.2.1   Fabrication of Wings and Pre-tensioning Method

Step 1.   A preexisting wing mold is used to construct the wing. A light coat of spray glue is applied.

Step 2.   Teflon film is laid on the mold for easy separation of the composite wing after the curing process is completed.

Step 3.   Two layers of 45° oriented bi-directional prepreg carbon fiber layers are cut out utilizing a template. Another layer of carbon fiber is cut out only for the leading edge for added strength.

Step 4.   A random speckling pattern is applied on one side of the silicone membrane while both sides are corona treated.

Step 5.   The perimeter of the silicone membrane is sandwiched between the layers of the composite. A picture is acquired by the VIC system as a reference image.

Step 6.   The entire assembly is vacuumed to be cured in the oven at 130°C for 4 h.

Step 7.   A similar procedure is followed for a batten reinforced wing, except that unidirectional carbon fiber is used for the construction of the battens. On Step 7 the silicone is tensioned and the final picture is obtained utilizing the VIC cameras for analysis. Five perimeter reinforced and two batten reinforced wings are manufactured for analysis and comparison; however, future work will involve a greater number of batten reinforced wings (Fig. 8.2).
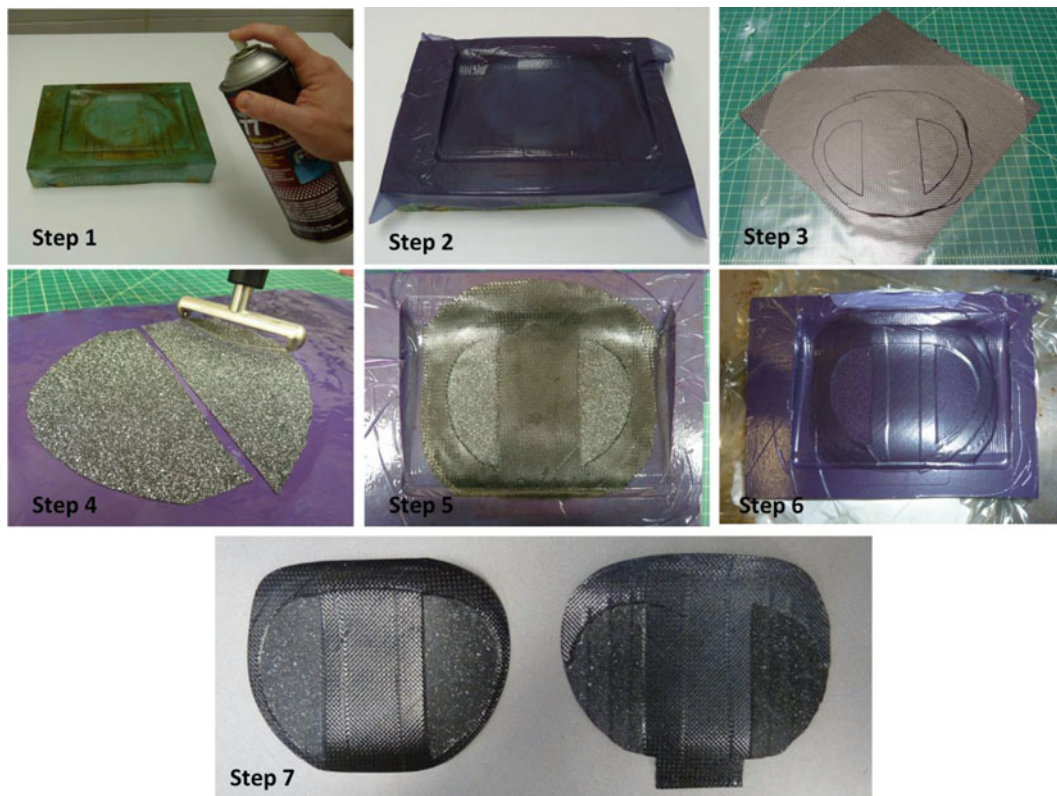

Fig. 8.2 Experimental steps involved in the construction and analysis of the MAV wings
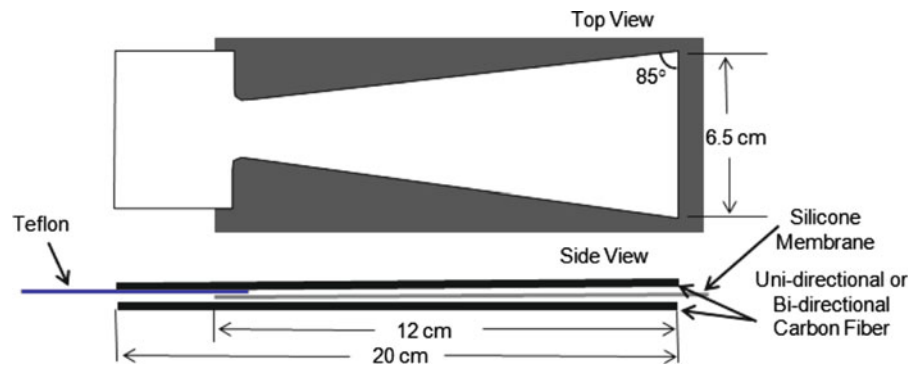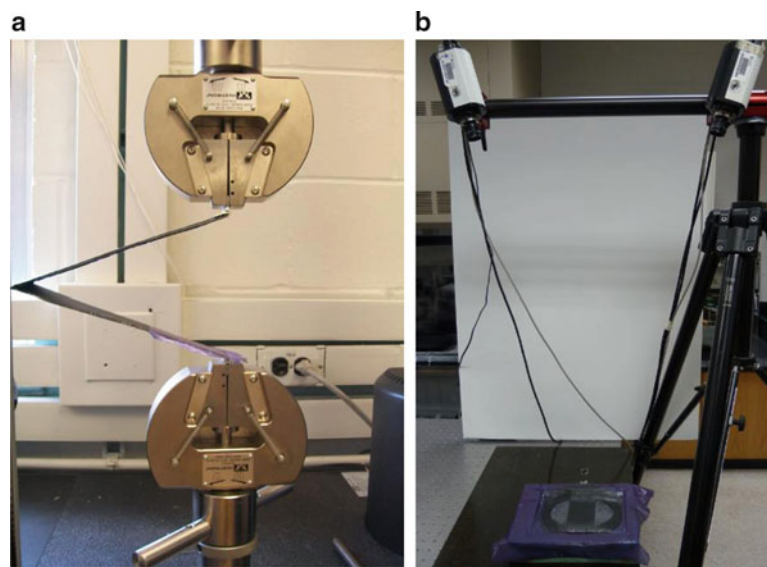
Fig. 8.3 Preparation of tapered double cantilever beam

Fig. 8.4 Experimental setup (**a**) analysis of the DCBT (**b**) analysis of the deformed silicone membrane

8.2.2 Fabrication of Width Tapered Double Cantilever Beam

The reasons for the choice of the width tapered double cantilever beams WTDCB specimen are discussed in the introduction. Four groups of WTDCB are manufactured according to the illustration shown in Fig. 8.3, each group containing six specimens: plain silicone with bi-directional and unidirectional carbon fiber and corona treated silicone with bi-directional and unidirectional carbon fiber. Silicone membrane is sandwiched between two six-layer carbon fiber composites. A thin film of Teflon is applied to initiate the crack at the starting point of the beam. Finally, the entire assembly is cured in the oven under vacuum pressure to be analyzed in the Instron machine.

8.2.3 Complete Experimental Arrangements for Analysis

The experimental setup for the testing of corona treatment consists of two hinges adhered on both sides of the double cantilever beam and hinges clamped on the two jaws of the Instron 5567 as seen on Fig. 8.4a. The Instron machine is capable of measuring loads up to 30 kN with maximum and minimum speeds of 500 mm/min and 0.001 mm/min respectively. The V-clamp design provides an increasing compression force on the hinges with an increasing vertical tensile force applied on the jaws to avoid slipping. Crack is initiated with a Teflon film while the crack length (mm) and the required force (N) are recorded as the jaws pull the two sides of the beam.

Table 8.1 Properties of silicone membrane

Property	Value (Unit)
Elastic modulus (E)	385 kPa
Poisson's ratio	0.43
Thermal expansion coefficient(CTE)	$2.8*10^{-4}$/C
Thickness	0.28 mm
Operating temperature range	$-62°C–218°C$

Figure 8.4b shows the arrangement to measure the strains developed on the speckled specimen with two VIC cameras connected to the computer through a DAC device. The cameras are calibrated to acquire pictures of the membrane before and after the curing of the carbon fiber.

8.2.4 Properties of Silicone Membrane

Abudaram et al. [9] calculated the elastic modulus and Poisson's ratio values experimentally utilizing the VIC system by hanging weights at the end of a long strip of silicone membrane (12:1 ratio) and recorded the strain values in the x and y directions. The values provided for the elastic modulus is calculated by curve fitting the data points according to the Eulerian approach. The thermal coefficient of expansion was computed in a similar manner by recording the temperatures with the infrared thermometer and strain values in x and y directions utilizing the VIC system. The thickness of the silicone membrane was measured with digital calipers while the operating temperature range was provided by the manufacturer (Table 8.1).

8.2.5 Visual Image Correlation System

All deformation will be measured with visual image correlation (VIC), a non-contacting full-field measurement technique originally developed by researchers at the University of South Carolina. The underlying principle is to calculate the displacement field of a test specimen by tracking the deformation of a random speckling pattern applied to the surface. Two pre-calibrated cameras digitally acquire this pattern before and after loading, using stereo-triangulation techniques. The VIC system then tries to find a region (in the image of the deformed specimen that maximizes a normalized cross-correlation function corresponding to a small subset of the reference image. The reference image is taken when no load is applied to the structure). The image space is iteratively swept by the parameters of the cross-correlation function to transform the coordinates of the original reference frame to coordinates within the deformed image. As it is unlikely that the deformed coordinates will directly fall onto the sampling grid of the reference image, accurate grey-value interpolation schemes are implemented to achieve optimal sub-pixel accuracy without bias.

The twin cameras are connected with a PC via an IEEE 1394 firewire cable, and a specialized unit is used to synchronize the camera triggers for instantaneous shots. A standard acquisition board installed in the computer carries out digitalization of the images, and the image processing is carried out by custom software, provided by Correlated Solutions, Inc. Typical data results obtained from the VIC system consist of geometry of the surface in discrete coordinates (x, y, z) and the corresponding displacements (u, v, w). The VIC system places a grid point every N pixels, where N is user defined. A final post-processing option involves calculating the in-plane strains (ε_{xx}, ε_{yy}, and ε_{xy}). This is done by mapping the displacement field onto an unstructured triangular mesh, and conducting the appropriate numerical differentiation, in which the complete definition of finite strains is used.

8.3 Results and Discussion

8.3.1 WTDCB Test for Corona Treatment

Separation speed on the Instron machine was set to 10 mm/s and average forces from crack initiation until the complete crack propagation are reported for all specimens on Table 8.2. Standard deviations on treated samples may have been caused by the application of the corona treatment: the amount of time, plasma charge distance and speed from the silicone surface,

Table 8.2 Average forces (n) recorded on all specimens

	Untreated unidirectional (N)	Treated unidirectional (N)	Untreated bidirectional (N)	Treated unidirectional (N)
Specimen #1	29.7	30.3	19.8	32.9
Specimen #2	21.1	33.9	18.8	22.0
Specimen #3	21.9	30.6	20.6	24.4
Specimen #4	30.5	29.7	20.0	NA[a]
Specimen #5	21.2	37.2	21.2	20.0
Specimen #6	32.2	30.7	18.9	21.9
Average	26.1	32.1	19.9	24.2
Standard Dev.	5.22	2.91	0.94	5.09

[a]Results for treated unidirectional specimen #4 are not reported on this table due to a manufacturing error
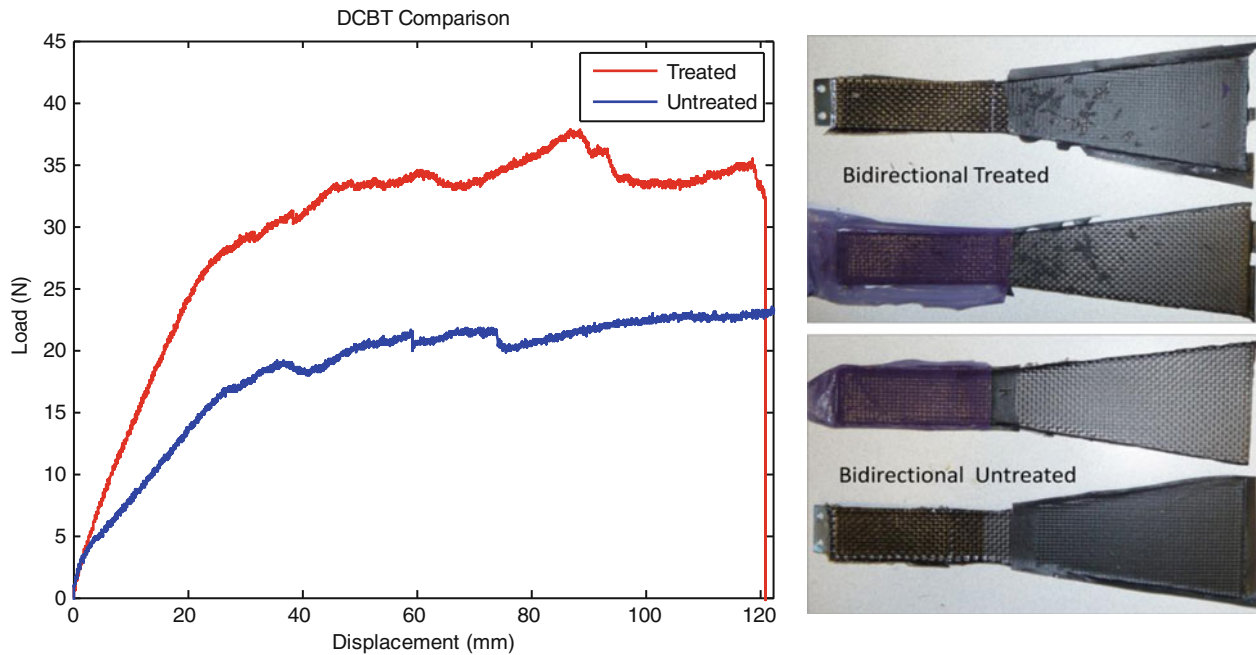

Fig. 8.5 WTDCB tests for corona treated and untreated silicone on bidirectional carbon fiber

uniform application on each specimen during the fabrication plays crucial role in the adhering process. The high deviation on untreated unidirectional specimens is probably due to the uneven thicknesses composite layers.

The data clearly shows that more energy is required to separate all corona treated specimens. Corona treated and untreated specimens with maximum averages are reported on Figs. 8.5 and 8.6 along with pictures after separation for further discussion. Untreated samples are separated in a much smoother fashion in comparison to corona treated samples. The dynamics involved in the detachment of corona treated samples are extremely complex due to adhesive and cohesive effects.

8.3.2 Membrane Pre-tensioning on Wing

Before acquiring pictures, the wing samples were waited to cool down to room temperature. Normal strains in x and y directions along with shearing strains are reported in Fig. 8.7 for a typical wing among five experiments. The strain resolution of the VIC system is estimated to be 500 $\mu\varepsilon$, a relatively high value (compared to strain gages, for example) due to the fact that the data is obtained by appropriately differentiating the displacement fields. The VIC system is not expected to have the resolution to capture the accurate strain information in the carbon fiber frame; therefore, only the membrane deformation was taken into account for calculations.

The membrane expanded due to the vacuum pressure and the high temperature in the oven. When cooled down to room temperature, the wing was naturally pretensioned. The anisotropy of strain is clearly evident from Fig. 8.7 as the wing has a
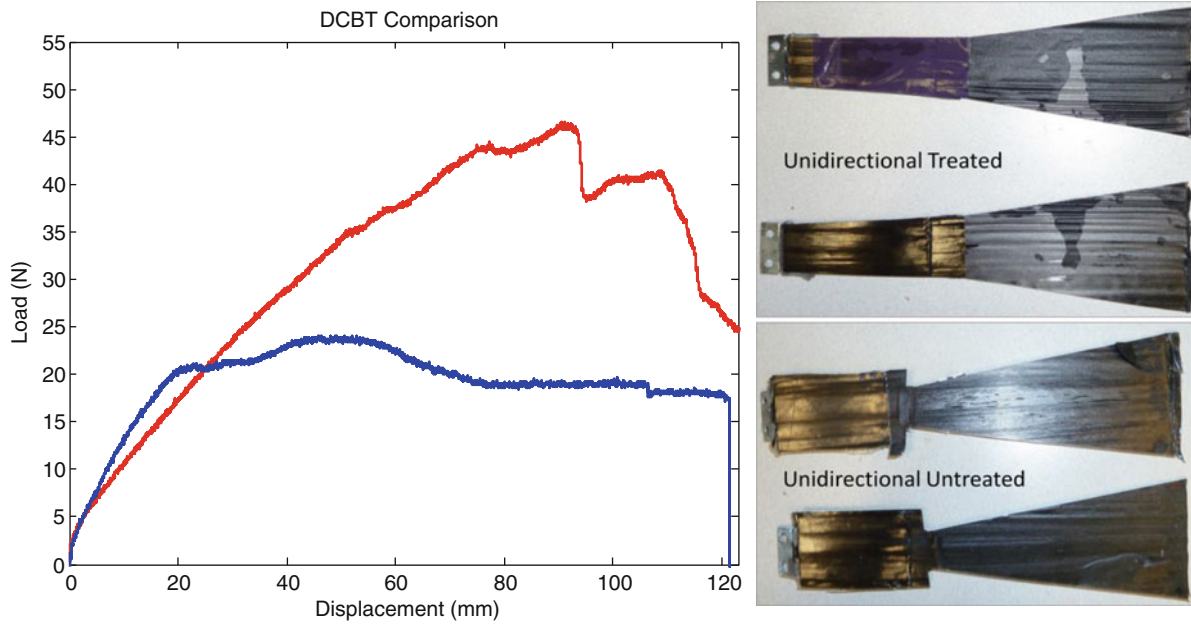
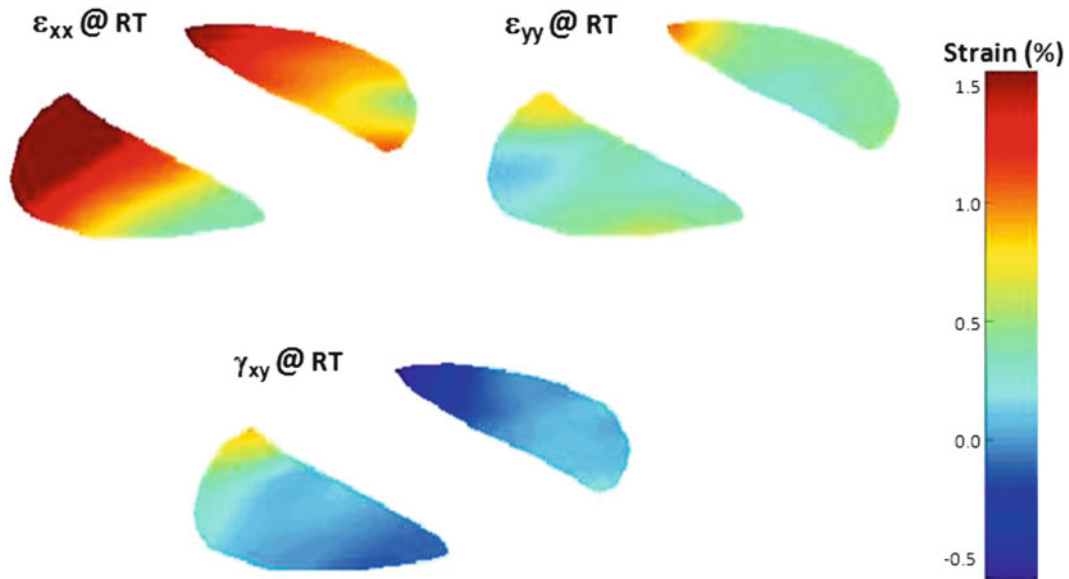**Fig. 8.6** WTDCB tests for corona treated and untreated silicone on unidirectional carbon fiber

Fig. 8.7 Acquired strain distribution on silicone membrane at the *bottom* of the perimeter reinforced wing

camber and the frame geometry is not symmetrical. Note that images on Fig. 8.7 show the bottom of the wing. Higher strains are computed toward the leading edge while this effect is muted toward the trailing edge for normal strains. Insignificant amounts of shear strains are recorded for all samples.

All strain values are then converted to stresses using the values on Table 8.1 as seen in Fig. 8.8. Stresses in normal directions range from approximately 3 kPa to over 9 kPa while much higher averages are recorded for stresses in x direction. This effect could be due to a shorter span in the chordwise direction in comparison to the longitudinal direction.

Average strains on the right and left sides of the five wings were calculated in x and y directions along with standard deviations as seen in Fig. 8.9. For each wing slightly higher strain values in the chordwise direction were measured and the highest standard deviation among all samples was calculated in this direction as well. The rest of the variations were within the same percentage, which shows the method is reasonably repeatable.
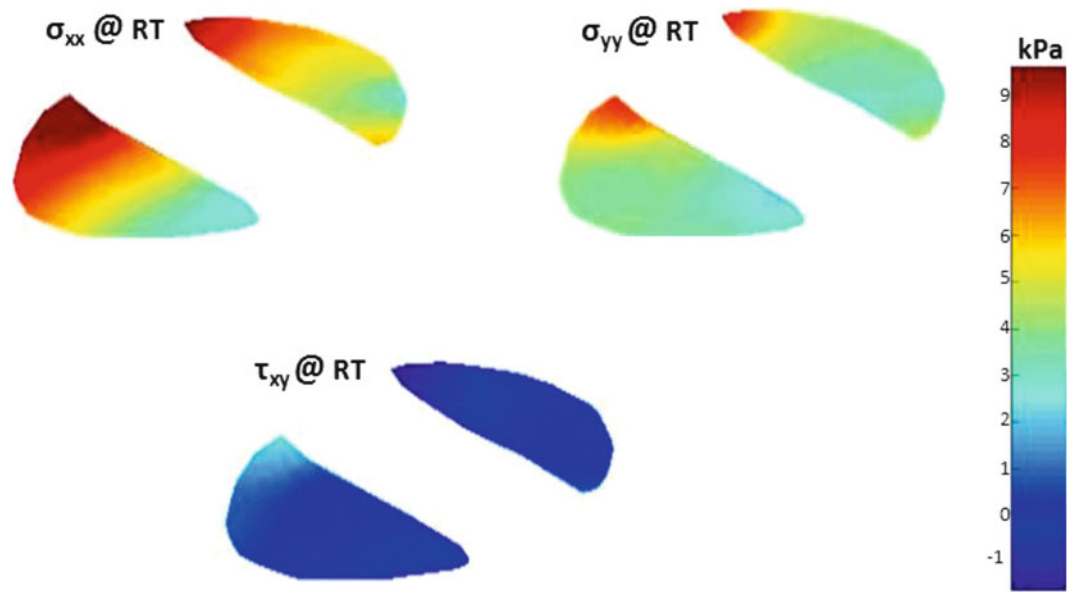
Fig. 8.8 Calculated pre-tension distribution on silicone membrane at the *bottom* of the perimeter reinforced wing
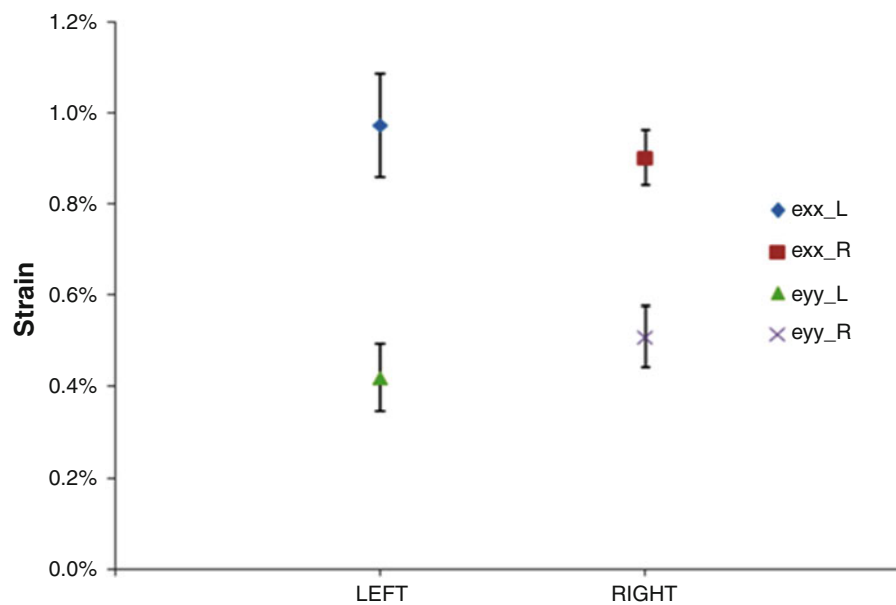

Fig. 8.9 Average strains developed on membrane in x and y directions on *left* and *right* hand side of perimeter reinforced wing

8.4 Conclusion

Various samples for corona treated and untreated silicone/carbon fiber specimens were manufactured. The samples were analyzed via Instron machine. The bonding technique is then applied to a series of MAV wings to be co-cured in the oven under vacuum pressure and the results are processed utilizing visual image correlation system:

1. When corona treated specimens were compared to their non-treated counterparts, the method showed a significant effectiveness in bonding.
2. Unidirectional carbon fiber specimens required more tensile force to separate whether they are treated or not.
3. The fabrication technique to build a wing with corona treated silicone membrane is explained.

4. VIC system showed the membrane is tensioned on both sides of the wing. The average strains were measured for all samples to show the repeatability.
5. The pretension was quantified via analysis.

Future work will involve results for batten reinforced MAV wings in a similar fashion. The wings may be cured at various temperatures to see the effect of temperature increase during the curing process on the strained developed at the room temperature.

References

1. Mueller TJ (2000) Proceedings of the conference on fixed flapping and rotary wing vehicles at very low Reynolds numbers, Notre Dame University, Indiana, 5–7 June 2000
2. McMichael JM, Col. Francis MS, USAF (1997) Micro air vehicles – toward a new dimension in flight from http://www.fas.org/irp/program/collect/docs/mav_auvsi.htm
3. Ifju PG, Ettinger S, Jenkins D, Martinez L (2001) Composite materials for micro air vehicles (MAV's). SAMPE J 37(4):7–12
4. Stanford B, Ifju P, Albertani R, Shyy W (2008) Fixed membrane wings for micro air vehicles: experimental characterization, numerical modeling, and tailoring. Prog Aerospace Sci 44:258–294
5. Pisano W, Lawrence D (2008) Autonomous gust insensitive aircraft. In: AIAA guidance, navigation, and control conference, Honolulu, 18–21 Aug 2008
6. Stanford B, Ifju P (2009) Aeroelastic topology optimization of membrane structures for micro air vehicles, structural and multidisciplinary optimization. doi: 10.1007/soo158-008-0292-x
7. Abudaram Y, Stanford B, Ifju P (2009) Wind tunnel testing of load-alleviating membrane wings at low reynolds numbers. In: Proceedings of 47th AIAA sciences meeting including the New Horizons Forum and aerospace exposition conference, Orlando, 5–11 Jan 2009
8. Stanford B, Sytsma M, Albertani R, Viieru D, Shyy W, Ifju P (2007) Static aeroelastic model validation of membrane micro air vehicle wings. AIAA J 45(12):2828–2837
9. Abudaram Y, Ifju PG, Hubner JP, Ukeiley L (2012) Controlling pre-tension of silicone membranes on micro air vehicle flexible wings. In: 50th AIAA sciences meeting, Nashville, 9–12 Jan 2012
10. Zhang D, Sun Q, Wadsworth LC (1998) Mechanism of corona treatment on polyolefin films. Polymer Eng Sci 38(6):965–970
11. Bikerman J (1967) Causes of poor adhesion: weak boundary layers. Ind Eng Chem 59(9):40–44
12. Joyoti A, Gibson RF, Newaz GM (2005) Experimental studies of mode I energy release rate in adhesively bonded width tapered composite DCB specimens. Compos Sci Technol 65:9–18
13. Daniel IM, Shareef I, Aliyu AA (1985) Rate effect on delamination fracture toughness of a toughened graphite/epoxy. American Soc Test, Houston, Texas,13-15 March 1985 937:260–274